Separation and Purification Technology 320 (2023) 124224

Contents lists available at ScienceDirect

Separation and Purification Technology

journal homepage: www.elsevier.com/locate/seppur

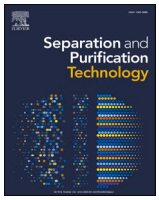

Pristine Multi-walled carbon nanotubes for a rapid and efficient plasmid DNA clarification

P. Ferreira [a], M. Riscado [a], S. Bernardo [a], M.G. Freire [b], J.L. Faria [c,d], APM. Tavares [b], CG. Silva [c,d], F. Sousa [a,*]

[a] CICS-UBI – Health Sciences Research Centre, University of Beira Interior, Av. Infante D. Henrique, 6200-506 Covilhã, Portugal
[b] CICECO – Aveiro Institute of Materials, Department of Chemistry, University of Aveiro, 3810-193 Aveiro, Portugal
[c] LSRE-LCM – Laboratory of Separation and Reaction Engineering – Laboratory of Catalysis and Materials, Faculty of Engineering, University of Porto, Rua Dr. Roberto Frias, 4200-465 Porto, Portugal
[d] ALiCE – Associate Laboratory in Chemical Engineering, Faculty of Engineering, University of Porto, Rua Dr. Roberto Frias s/n, 4200-465 Porto, Portugal

ARTICLE INFO

Keywords:
Gene therapy
Carbon nanotubes
Plasmid DNA isolation
RNA

ABSTRACT

Therapeutic approaches based on nucleic acids to modulate cell activity have recently gained attention. These molecules arise from complex biotechnological processes, requiring effective manufacturing strategies, high purity, and precise quality control to be used as biopharmaceuticals. One of the most critical and time-consuming steps for nucleic acids-based biotherapeutics manufacturing is their purification, mainly due to the complexity of the extracts. In this study, a simple, efficient, and reliable method to isolate and clarify plasmid DNA (pDNA) from complex samples is described. The method is based on the selective capture of RNA and other impurities, using pristine carbon nanotubes (CNTs). Multi-walled CNTs (MWCNTs) with different diameters were studied to determine their adsorption capacity and to address their ability to interact and distinguish between nucleic acids. The results revealed that MWCNTs preferentially interact with RNA and that smaller MWCNTs present a higher adsorption capacity, as expected by the higher specific surface area. Overall, this study showed that MWCNTs significantly reduce the levels of impurities, namely RNA, gDNA, and proteins, by approximately 83.6 % compared to their initial level, enabling the recovery of clarified pDNA in solution while maintaining its stability throughout the recovery process. This method facilitates the pre-purification of pDNA for therapeutic applications.

1. Introduction

Friedmann and Roblin envisioned using exogenous functional gene copies to treat genetic disorders over 50 years ago [1]. Since then, nucleic acids-based therapies have gained prominence, being at the forefront of global efforts to fight the COVID-19 pandemic [2,3]. Several strategies for DNA-based therapy have been approved, and numerous clinical trials are currently ongoing [4]. The main therapeutic indications comprise cancer [5], allergies [6], autoimmune [7], and infectious diseases [8,9]. The biocompatibility, cost-effective production, and long shelf-life, provide DNA-based therapies with a promising future in personalized medicine [10].

Due to the rising interest in the application of pDNA in vaccines and gene therapy, an increased demand for this type of product has emerged, and thus, plasmid biomanufacturing must become more effective, with improved productivity [11]. One of the most critical steps for pDNA manufacturing for biomedical applications is its isolation and purification [12]. To date, several unit operations should be arranged for the separation and purification of pDNA-based biopharmaceuticals, with the primary goal of removing impurities associated with recombinant production [12]. This process undertakes several challenges, primarily due to the diversity of biomolecules derived from the producer host. Usually, the starting material consists of complex lysates from bacterial cells resulting from alkaline lysis, where no more than 3 % represents pDNA. The remaining 97 % consists of impurities, like RNA, gDNA, open circular pDNA, and endotoxins, presenting some similarities to pDNA [13].

At laboratory-scale the conventional methods for isolation and purification of pDNA present significant drawbacks, since they often require animal-derived enzymes, toxic chemicals or organic solvents

* Corresponding author.
E-mail address: fani.sousa@fcsaude.ubi.pt (F. Sousa).

https://doi.org/10.1016/j.seppur.2023.124224
Received 31 January 2023; Received in revised form 24 May 2023; Accepted 26 May 2023
Available online 27 May 2023

[14], namely RNase, proteinase K, phenol and/or chloroform [15]. Large-scale purification processes are predominantly based on chromatographic methods. Although versatile and with high resolution, chromatographic methods still pose some challenges due to low binding capacity and slow mass transfer, mainly driven by the pDNA size [16]. Furthermore, these methods are heavily time-consuming and highly dependent on the upstream process and prior-downstream steps [17]. Thus, it is essential to exploit efficient, accurate, sensitive, selective, and easy-to-operate purification techniques [18]. Among recent developments for DNA isolation, solid-phase extraction (SPE) has gained relevance (Table 1) by providing a fast and efficient purification step. It enables the pre-concentration of samples, avoiding the use of volatile and dangerous organic solvents [19,20]. CNTs also attracted particular interest as a novel SPE material and are promising alternatives to improve the current protocols. Owing to their unique properties, nanomaterials, like CNTs, are expected to provide solutions to challenges in a wide range of fields, from biomedical applications to environmental sciences [21–24].

CNTs are composed of graphene sheets rolled up to form tubular, needle-shaped structures with nanometric scale in diameter and several millimeters in length. Because each atom of carbon has three neighborhoods, CNT has a strong bond between C–C atoms (sp^2 hybridization), making them very stable against deformations [25]. Therefore, CNTs present high aspect ratio, high specific surface area, high tensile strength, low mass density, and exceptional adsorption properties [26,27]. Even when comparing with other similar materials, such as other carbon materials, CNTs possess exceptional specific surface area-to-volume ratio, unique nanotubular structure, and long lifetime, which contribute to enhanced adsorption efficiency [28]. In this regard, CNTs are already being studied as an alternative for acting as adsorption material to recover dyes [29], pharmaceuticals [30], heavy metals [31], proteins [32], and nucleic acids [33].

Most strategies reported in the literature employing CNTs as adsorption supports rely on surface modifications. In one approach, Fe_3O_4-magnetized MWCNTs coated with a poly(ethylene glycol)-based deep eutectic solvent were used for DNA extraction [33]. Coating the MWCNTs increased the adsorption capacity from approximately 50 to 178 mg/g, significantly improving the method's performance. Although surface modifications can improve the dispersibility and adsorption capacity, this process undergoes a series of steps, making it laborious and time-consuming.

This work presents a simple strategy to isolate and clarify pDNA from complex lysate samples by using pristine MWCNTs without surface modification. The MWCNTs are used for the adsorption of impurities, such as RNA, proteins, and gDNA. This strategy is rapid and efficient and does not require adsorption and desorption steps of the target molecule, preventing material loss during the procedure. To characterize the adsorption capacity, MWCNTs with different diameters were evaluated. Different types of interactions were studied to address the selective interaction between pristine MWCNTs and RNA. After the clarification procedure, pDNA stability and integrity were confirmed. *In vitro* tests assessed the cytotoxicity of MWCNTs to prove that the developed depuration can be safe upon processing these potential biopharmaceuticals. This work provides new insights for pDNA isolation and RNA capture by pristine MWCNTs, describing a new, rapid, and effective protocol for pDNA purification at a laboratory scale.

Table 1
An overview of reported methods to isolate and extract nucleic acids.

Materials	Extraction capacity (mg/g)	Molecule adsorbed	References
PEI-$FePO_4$	61.88	DNA	[34]
DES-mCS/MWCNTs	177.66		[33]
IL-Fe_3O_4	19.80		[14]
APBA attached-silica microspheres	60	RNA	[35]
Poly(HEMA-co-VPBA)	16		[36]
GO-MPs	74.6		[37]

(PEI – Polyethyleneimine; DES-mCS/MWCNTs – Deep eutectic solvent-chitosan-modified Fe_3O_4-magnetized multi-walled carbon nanotubes; IL – Ionic liquid; APBA – 3-aminophenylboronic acid; HEMA – 2-hydroxyethylmethacrylate; VPBA – 4-vinylphenylboronic acid; GO – Graphene oxide; MPs – Magnetic particles.).

2. Materials and methods

All chemicals and reagents used were of analytical grade. Experiments were performed with MWCNTs with different diameters purchased to Shenzhen NTP, China. The MWCNTs properties are described in Table 2. Experiments were performed with ammonium sulfate ($(NH_4)_2SO_4$), commercialized by Panreac (Barcelona, Spain), and tris (hydroxymethyl)aminomethane (Tris) from Merck (Darmstadt, Germany). The pDNA purification kit, NZYMaxiprep, was from NZYTech (Lisbon, Portugal). The purity of pDNA was evaluated using a CIMac™ pDNA 0.3 mL analytical column from BIA Separations (Ajdovščina, Slovenia). Normal human dermal fibroblast (NHDF) adult donor cells, Ref. C-12302 (cryopreserved cells) were purchased from PromoCell (Middlesex, UK). All solutions were freshly prepared using ultra-pure grade water, purified with a Milli-Q system from Merck Millipore (Darmstadt, Germany). All the experiments were performed at room temperature (RT) and repeated at least 3 times.

2.1. Bacterial growth and nucleic acids production

RNA was obtained from an *E. coli* DH5α strain culture, previously transformed with the plasmid pBHSR1-RM containing the human sequence of pre-miR-29b [38]. For the assays where cell lysate was required, an *E. coli* DH5α strain with 6.07 kbp pcDNA3-FLAG-p53 Addgene plasmid 10,838 [39] (Addgene, USA) containing a human sequence of p53 was used. The detailed procedure and bacterial growth conditions are available in the Supporting Information.

2.2. Alkaline lysis and nucleic acid extraction

In this study, three types of nucleic acid samples were used, being obtained by different extraction methods: (1) a lysate sample comprising pDNA, gDNA, RNA, and proteins, obtained by a procedure based on a modified alkaline lysis, as described by Diogo *et al.* [40]. For this process, no toxic solvents, or animal-origin enzymes were used, and no alcohol precipitation was required before the capture step. After cell lysis, pristine MWCNTs were applied to remove RNA, proteins, and gDNA fragments from the *E. coli* lysate, as described in section 2.3; (2) a low molecular weight RNA sample, obtained by the acid guanidinium thiocyanate-phenol–chloroform method [41]. In this protocol, the RNA sample is finally obtained by resuspension in 1 mL of DEPC-treated water and left to rehydrate at RT for 15 min to ensure complete solubilization; (3) a pDNA sample, obtained by the NZYMaxiprep kit (NZYTech, Portugal), according to the protocol provided by the manufacturer. The concentration of RNA and pDNA samples were determined

Table 2
General MWCNTs characteristics (supplier data).

Model	OD	Length	Purity	ASH	SSA
<10 MWCNT	7–10 nm	>5 μm	>97 %	<3 wt %	250 ~ 500 m^2/g
<10/20 MWCNT	10–20 nm	>5 μm	>97 %	<3 wt %	100 ~ 160 m^2/g
20/40 MWCNT	20–40 nm	>5 μm	>97 %	<3 wt %	80 ~ 140 m^2/g
60/100 MWCNT	60–100 nm	>5 μm	>97 %	<3 wt %	40 ~ 70 m^2/g

(OD – Outer diameter; ASH – Ash content; SSA – Specific surface area.).

with a NANOPhotometer (Implen) at 260 nm, and their integrity and purity were routinely assessed by 1 % agarose gel electrophoresis.

2.3. Solid-phase extraction using MWCNTs

SPE was applied to capture RNA and other impurities from complex *E. coli* lysates using pristine MWCNTs. Several strategies and conditions were optimized until an efficient method was established. Fig. 1 represents the whole process developed in this work.

This method comprises two main steps: (1) the equilibration step, where 1 mg of pristine MWCNTs was equilibrated with an optimized equilibration buffer, followed by 20 min of agitation and posterior centrifugation at 8000 g for 2 min to remove the aqueous phase and recover the equilibrated MWCNTs. The samples to be applied onto the MWCNTs (lysate samples or pre-purified RNA or pDNA used as control samples) were also diluted within the same equilibration buffer; (2) the adsorption step, where the sample was put in contact with the MWCNTs to promote adsorption of some species. The mixture was kept at RT (approximately 25 ℃), in agitation, for 20 min to allow nucleic acid adsorption onto MWCNTs. Then, another centrifugation at 8000 g for 2 min was performed to separate the solid phase from the aqueous phase. The supernatant was recovered to analyze nucleic acid concentration, integrity, and purity. Different sample compositions and buffers were used in this work, mainly varying the pH, type of salt, and concentration used in the equilibration/adsorption buffers, as detailed in the "Results" section.

2.4. Purity analysis

The pDNA quality control requires the assessment of specific impurities, such as RNA, proteins, and gDNA, present in purified pDNA samples. Those were assessed by different techniques, as detailed below.

2.4.1. Agarose gel electrophoresis

Nucleic acids analysis, regarding the evaluation of the identity and relative purity of different samples, was continuously performed by agarose gel electrophoresis in 1 % agarose gel. Nucleic acids were stained in the gel with Green Safe (0.012 µL/mL), and electrophoresis was run at 120 V for 30 min in TAE buffer (40 mM Tris base, 20 mM acetic acid, and 1 mM EDTA, pH 8.0). The gels were visualized under ultraviolet (UV) light exposure with a UV chamber (UVITEC Cambridge, Cambridge, United Kingdom).

2.4.2. Analytical chromatography

The purity and recovery of pDNA were evaluated using a CIMac™ pDNA 0.3 mL analytical column (BIA Separations, Slovenia). For the chromatographic experiments, the analytical column was connected to an ÄKTA Purifier system (GE Healthcare Biosciences), and an adequate gradient was established, as described in the Supporting Information.

2.4.3. Protein quantification

Standard Bio-Rad Protein Assay (Bio-Rad, California, USA) was used to determine the total protein concentration in the *E. coli* lysate samples, before and after clarification, according to the manufacturer's instructions. The calibration curve was designed, using bovine serum albumin (BSA) as a protein standard, in the linear range from 0.05 to 0.5 mg/mL.

2.4.4. Genomic DNA quantification

For quantitative analysis of gDNA present in the purified samples, real-time polymerase chain reaction (qPCR) was performed in 96-well optical plates, using the Maxima® SYBR Green/Fluorescein qPCR Master Mix (2X) (Thermo Fisher Scientific Inc.) in a CFX Connect™ Real-Time PCR Detection System (BioRad). A calibration curve was determined with gDNA concentrations varying from 0.005 to 50 ng/µL and by correlating the quantitation cycle (Cq) and the logarithm of gDNA concentration. All reactions were performed in triplicate, and Cq values were averaged. The specific 16 s ribosomal RNA (rRNA) primer sequence and amplifications conditions are described in the Supporting Information.

2.5. Circular dichroism spectroscopy

Circular Dichroism (CD) experiments were performed to assess the structural stability of pDNA after the clarification procedure with MWCNTs. CD was performed using a Peltier-type temperature control system in a Jasco J-815 spectropolarimeter (Jasco, Easton, MD, USA). The CD signal was converted to ellipticity. Three scans were measured per spectrum to improve the signal-to-noise ratio, and the spectra were smoothed using the smooth tool in OriginPro 2018 software. Details about the CD spectra acquisition are available in the Supporting Information.

2.6. Determination of pristine MWCNTs cytotoxicity by 3-[4,5-dimethylthiazol-2-yl]-2,5-diphenyltetrazolium bromide (MTT) assay

NHDF cells were used for the cytotoxicity evaluation of < 10 MWCNTs. NHDF cells at passages 10–20 were seeded in DMEM-F12 medium (Sigma-Aldrich) supplemented with 10 % (w/v) FBS heat-inactivated and 1 % (w/v) penicillin–streptomycin, at a density of $1x10^4$ cells per well in a 96-well plate. After 24 h the medium was replaced by a new medium and 25, 50, and 100 µg of MWCNTs were added to each well. The cytotoxicity was evaluated at different time points, namely 24 and 48 h with the Cell Proliferation Kit I (MTT) assay, according to the protocol provided by the manufacturer. All experiments were done in triplicate using independent culture preparations, and positive control cells were treated with 70 % ethanol. The information regarding the data analysis can be found in the Supporting Information.

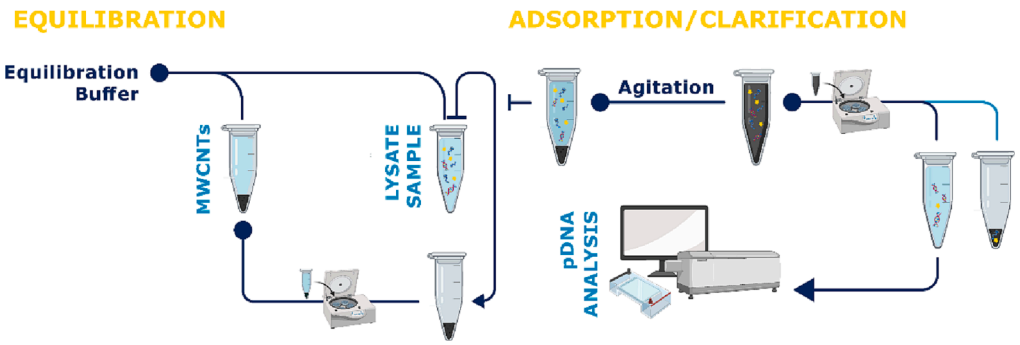

Fig. 1. Schematic representation of pDNA clarification from complex lysates using MWCNTs.

3. Results and discussion

3.1. Screening of adsorption conditions

Adsorption of RNA and pDNA on MWCNTs with different diameters were screened using experimental conditions that could mainly promote electrostatic or hydrophobic interactions when applying 50 μg of RNA or pDNA. This study allows an understanding of the influence of these parameters in nucleic acid capture and adsorption, enabling the identification of the main interactions between MWCNTs and these molecules.

As depicted in Fig. 2, a higher RNA adsorption on MWCNTs was achieved (greater than60 %) when ammonium sulfate was added to the binding buffer, a condition usually established for promoting hydrophobic interactions [42]. On the other hand, in the absence of salt, a low RNA adsorption capacity was observed (<40 %) for all MWCNTs diameters. This result proves that the RNA adsorption onto MWCNTs is mainly driven by hydrophobic interactions, which was already expected considering the hydrophobic character of MWCNTs [43]. The relatively hydrophobic surface of MWCNTs is more prone to promote hydrophobic interactions with the exposed nucleotide bases of RNA.

Considering that the RNA adsorption mainly occurred in the presence of ammonium sulfate, the ionic strength of the binding buffer was also evaluated to verify its effect on the adsorption of RNA onto MWCNTs. By increasing the concentration of ammonium sulfate of the binding buffer from 1.5 M $(NH_4)_2SO_4$ in 10 mM Tris-HCl pH 8 to 2.5 M $(NH_4)_2SO_4$ in 10 mM Tris-HCl pH 8.0, it was not observed a significant increase in RNA binding (results not shown). Therefore, this option was discarded for further studies.

Regarding the diameters of MWCNTs, the results revealed that the adsorption is higher for the MWCNTs with smaller diameters (Fig. 2). When comparing the RNA adsorption, there is a significant increase from 69 % to 94 % when changing the MWCNTs diameter from 10 to 20 nm to < 10 nm. This behavior was expected due to the higher specific surface area of the MWCNTs with smaller diameters (Table 2), resulting in higher availability of active sites for RNA adsorption. Due to the remarkable adsorption behavior, only the MWCNTs with diameters lower than 10 nm were considered for the subsequent studies.

When assessing the adsorption of pure pDNA onto MWCNTs, at the optimal conditions established for RNA adsorption, it was clear that pDNA did not interact with the surface of the MWCNTs, as depicted in the chromatogram shown in Fig. 3. This analysis was performed with a CIMac™ analytical column, where a pre-purified pDNA sample was loaded before and after the MWCNTs adsorption assay. Since the two peaks maintain somewhat the same shape and size, it can be concluded that no significant amount of pDNA was captured by the MWCNTs. These results also suggested that the selectivity between RNA and pDNA could potentially be achieved in these conditions. A more detailed analysis of the selectivity between these two molecules is described in section 3.3.

3.2. MWCNTs adsorption capacity

As the adsorption sites of MWCNTs are limited, becoming saturated at a certain RNA adsorption level, this assay was performed to evaluate the total RNA amount that the MWCNTs could capture. The experiment was carried out under the optimal adsorption conditions previously determined, namely by using 1.5 M $(NH_4)_2SO_4$ in 10 mM Tris-HCl, pH 8, as a binding buffer. Fig. 4 shows that the highest adsorption capacity is approximately 175 mg RNA/g MWCNTs. When loading 200 μg of RNA onto 1 mg of MWCNTs, around 29.7 μg of RNA was not adsorbed, suggesting that the adsorption capacity of the MWCNTs was reached.

According to the literature, SPE-based methods used to isolate and extract nucleic acids present different adsorption capacities, ranging from 16 to 74.6 mg/g when referring to RNA [14,33–37] and from 19.8 to 177.7 mg/g for DNA [14,33–37,44] (Table 1). Fu *et al.* (2021) conducted a study in which graphene oxide functionalized magnetic particles (GO-MPs) were prepared and used for RNA removal with the final goal of pDNA clarification, reaching a maximum RNA adsorption capacity of 74.6 mg/g. Also, Kip *et al.* (2019) investigated the affinity isolation behavior of RNA by using APBA attached-silica microspheres as the sorbent, obtaining a maximum RNA adsorption of 60 mg/g. In general, when compared with other adsorbents for RNA capture, the extraction capacity of 175 mg/g achieved herein with < 10 MWCNTs is significantly higher (Table 1). Overall, it is shown that this method has great potential to be used in pDNA clarification since it is extremely straightforward to apply, not resorting to additional chemical functionalization. Indeed, even when compared with DNA capture methods, MWCNTs show comparable extraction to other published adsorbents [14,34].

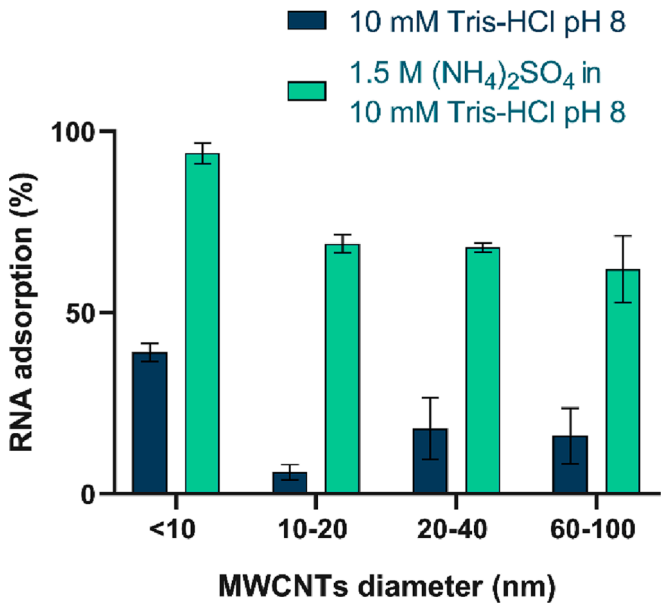

Fig. 2. RNA adsorption onto MWCNTs with different diameters using different binding conditions. Values were calculated with the data obtained from three independent measurements (mean ± SD, n = 3).

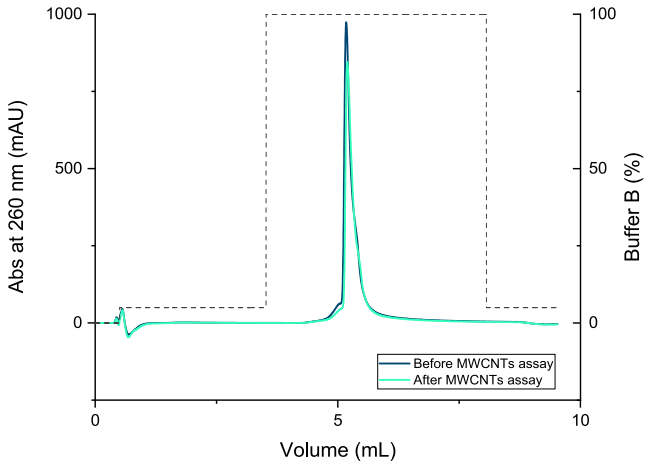

Fig. 3. Representative chromatograms of pDNA before and after contact with MWCNTs (<10 nm). Buffer A – 0.6 M NaCl in 100 mM Tris-HCl pH 8.0; Buffer B: 1 M NaCl in 100 mM Tris-HCl pH 8.0.

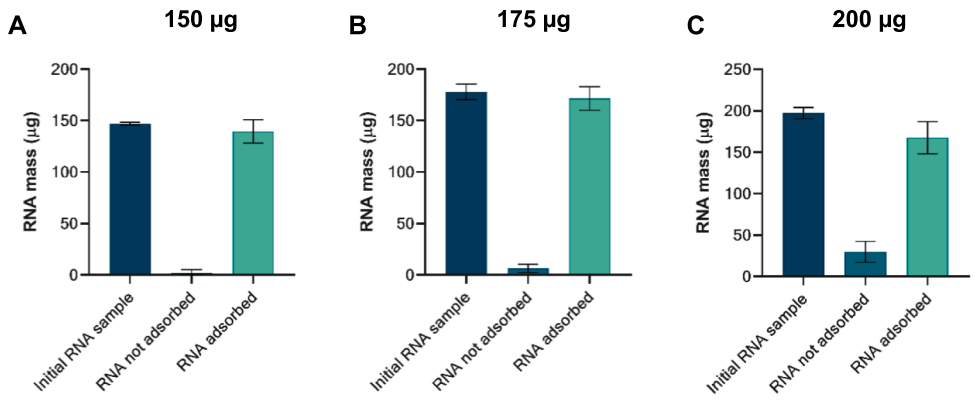

Fig. 4. RNA adsorption capacity of < 10 MWCNTs; A. Sample containing 150 µg of RNA/mg MWCNTs; B. Sample containing 175 µg of RNA/mg MWCNTs; C. Sample containing 200 µg of RNA/mg MWCNTs. Values were calculated with the data obtained from three independent measurements (mean ± SD, n = 3).

3.3. Selectivity to RNA or pDNA

Additional experiments were performed to evaluate the effective separation between RNA and pDNA. First, artificial mixtures comprising different ratios of RNA and pDNA were used. RNA and pDNA mixtures were prepared with a final concentration of 500 µg/mL (Fig. 5A) combined in three different ratios: 25 % RNA / 75 % pDNA; 50 % RNA / 50 % pDNA; 75 % RNA / 25 % pDNA. Through the analysis of the agarose gel electrophoresis (Fig. 5A), it was possible to observe that the concentration of both DNA and RNA does not influence the effectiveness of RNA capture, and even when a small concentration of RNA is present in the sample, the pDNA is not adsorbed onto MWCNTs. Important to note that the resulting samples were then submitted to a second adsorption cycle (Fig. 5A-F2) since not all RNA was captured in the first cycle due to MWCNTs saturation. This second cycle proved effective at removing the remaining RNA completely, contributing to improved clarification of the pDNA without compromising selectivity.

To further validate the selectivity of MWCNTs towards RNA adsorption, a complex *E. coli* lysate sample was used under the established conditions. Through the analysis of the agarose gel electrophoresis and comparing the initial lysate (Fig. 5B-S1) with the clarified sample obtained after an MWCNTs adsorption cycle (Fig. 5B-F1), it is observed that the RNA initially present in the lysate was mainly adsorbed onto MWCNTs, as the RNA band intensity (in lanes F1) is significantly lower than the RNA band in the lysate (Fig. 5B-S1). In contrast, pDNA was not captured by MWCNTs, as no difference in the pDNA band intensity was achieved after the adsorption cycle. This result proves that MWCNTs present selectivity for capturing contaminating RNA, even in more complex samples. That also confirms the possibility of using pristine MWCNTs for the clarification of pDNA samples.

Nevertheless, as the lysate is a very complex sample, the concentration of RNA is higher than the adsorption capacity of MWCNTs. The direct loading of the lysate leads to the MWCNTs overload and saturation, thus explaining why some of the RNA remains in the clarified sample (Fig. 5B-F1). Hence, to verify if it was possible to increase the purity of pDNA further, the first clarified sample (F1) was subjected to two additional capture cycles, completing a total of three cycles, i.e., the supernatant (non-adsorbed sample) resulting from the first cycle was applied in a second cycle, and the sample resulting from the second cycle was used in a third run (Fig. 6).

With this experiment, it was possible to determine the potential of MWCNTs to remove RNA from a complex sample thoroughly. The procedure optimized in this work can be helpful to substantially improve the purity of the pDNA sample since the decrease of RNA contamination is evident after each adsorption cycle (Fig. 5B). Thus, with only three adsorption cycles (Fig. 5B-F3), MWCNTs were able to capture all RNA

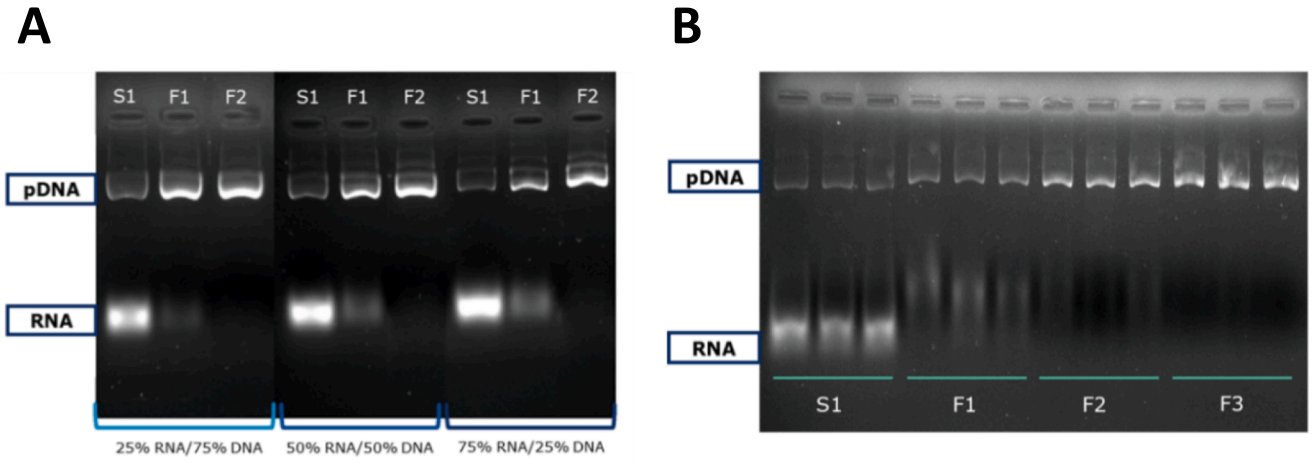

Fig. 5. A. Agarose gel electrophoresis of RNA and DNA artificial mixtures (in different proportions but completing 500 µg/mL) before and after < 10 MWCNTs adsorption. S1 - Initial sample; F1 - Sample after first adsorption cycle, comprising all solutes not adsorbed to MWCNTs; F2 - Sample after second adsorption cycle containing all lysate solutes not adsorbed to MWCNTs. B. Agarose gel electrophoresis of *E. coli* lysate before and after < 10 MWCNTs adsorption procedure for three consecutive cycles of adsorption (n = 3). S1 - Initial *E. coli* lysate sample subjected to the first adsorption cycle; F1 - Supernatant recovered from the first cycle, comprising all solutes not adsorbed onto MWCNTs; F2 - Supernatant recovered after the second cycle, containing all solutes not adsorbed onto MWCNTs; F3 - Supernatant recovered after the third cycle, comprising all solutes not adsorbed onto MWCNTs.

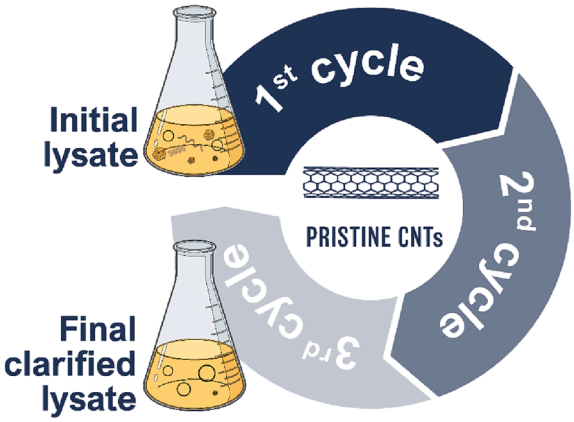

Fig. 6. Overview of the clarification process, where the lysate is subjected to three consecutive adsorption cycles using pristine MWCNTs.

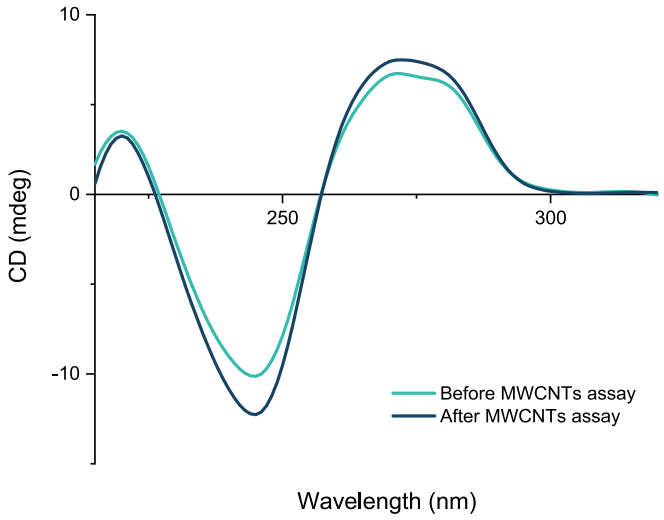

Fig. 7. CD spectra of pDNA before and after MWCNTs clarification assay.

present in the *E. coli* lysate sample, improving the pDNA purity. The selectivity shown by MWCNTs for RNA adsorption over pDNA can be explained by the fact that the nucleotide bases in RNA are more exposed than the DNA bases, which are organized in a double chain. This agrees with the results obtained by Nandy, *et al.* (2012), who showed that ssDNA and dsDNA interact differently with CNTs, being observed that ssDNA could wrap around CNTs surface and adsorb strongly, while dsDNA only adsorbed when partial unzipping of the chain occurred. Moreover, when assessing the interaction between siRNA and CNTs, Nandy and colleagues saw that siRNA unzipped the two strands, wrapping around the CNTs surface [45]. Consequently π-cloud of MWCNTs surface will have superior access to the hydrophobic bases of RNA, establishing more effective π-π interactions. Theoretically, these would make the pristine CNTs present poorer affinity to diverse types of molecules [18]. But, on the contrary, this feature was exploited in this work to achieve high selectivity between RNA and pDNA due to the different levels of nucleotide bases exposure, allowing π-π interactions between MWCNTs and RNA to be more effective. Hence, the more hydrophobic nature of RNA ultimately promotes more effective retention in CNTs, leading to the selective adsorption of RNA into MWCNTs and enabling pDNA clarification. Nevertheless, the strong interactions established between RNA and MWCNTs make the desorption of RNA a very challenging task and thus it was not possible to completely desorb the RNA while maintaining its integrity (results not shown). Even though the primary goal of the work performed is to establish a rapid and easy-to-operate pDNA clarification method, the desorption of RNA could be an important area to focus research on future works.

3.4. Clarified pDNA quality control

The integrity and structural stability of the clarified plasmid DNA recovered from the MWCNTs clarification procedure were studied by circular dichroism (CD). A pDNA control sample, purified with a commercial kit, was also analyzed for comparison purposes. Fig. 7 shows that both spectra have a similar profile with a negative band around 245 nm and two positive bands at 220 and 275 nm, which are the characteristic bands of DNA, corresponding to π-π base stacking and DNA helicity. The results indicate that no significant alterations in the secondary structure of pDNA occur during the clarification process with MWCNTs. Hence, the procedure does not compromise pDNA integrity, allowing it to maintain its native conformation.

The full potential of MWCNTs to remove impurities was evaluated by determining the purity of the clarified pDNA resulting from the adsorption process. This analysis was performed with a CIMac™ analytical column, where the initial *E. coli* lysate and the resulting pDNA-containing samples, recovered from each clarification cycle, were loaded. From the analysis of the electrophoretic bands corresponding to the peaks obtained in the chromatograms (Fig. 8), it was verified that the first and second peaks comprise the impurities, while the third peak represents the elution of pDNA (Fig. 8A). The chromatographic profiles and the electrophoresis demonstrate the impressive removal of most impurities along the 3 adsorption cycles. That was shown by the gradual reduction of peaks 1 and 2 in the chromatograms (Fig. 8A) and the elimination of the RNA bands in the electrophoresis (Fig. 8B). Moreover, looking at the pDNA peak profile (peak 3), it is verified that there is no significant change in the peak area, suggesting that the recovery yield of pDNA is also maintained throughout the three cycles.

Once completed this general characterization for the clarification of pDNA along the three adsorption cycles with MWCNTs, a more specific analysis was made, namely by quantifying the residual proteins and gDNA. It is reported that *E. coli*, the host used for pDNA production in this work, comprises around 4300 protein-coding genes [12]. Given this diversity, the removal of these biomolecules must be considered since they pose some risks and can induce immunogenic responses upon administration of biopharmaceuticals [46]. Several studies have shown the capability of CNTs to adsorb proteins [47]. In this regard, the quantification of proteins was also performed to verify if these impurities were mainly captured by the MWCNTs, as RNA or if they were maintained in solution with pDNA. The results suggested that a significant part of the total protein content was captured by the pristine MWCNTs, as the initial concentration in the lysate decreased from 128.5 μg/mL to 27.3 μg/mL after the first adsorption cycle. Moreover, the subsequent cycles also effectively removed the proteins, reaching a concentration of 5.4 μg/mL after the third cycle, finally corresponding to 96 % protein removal (Table 3).

Host DNA is also an essential concern for regulatory agencies and the biopharmaceutical industry. The main apprehension here is that residual fragments of foreign gDNA can be inserted into the patient's genome [12], which is of the utmost importance for removing this molecule from the pDNA biopharmaceutical sample. In this context, quantification of gDNA present in the complex lysate and in the sample recovered from the clarification step with MWCNTs was performed by qPCR. The results presented in Table 3 show that the clarification procedure reduces the levels of gDNA from 523.3 μg/mL, in the initial sample, to 90.0 μg/mL, after the third cycle, corresponding to a gDNA removal percentage of approximately 83 %.

To improve this result, a five-cycles clarification procedure was attempted, also increasing the amount of MWCNTs (2 mg) to be used on adsorption. However, none of these strategies significantly improved the final pDNA purity (results not shown), so these options were not further considered.

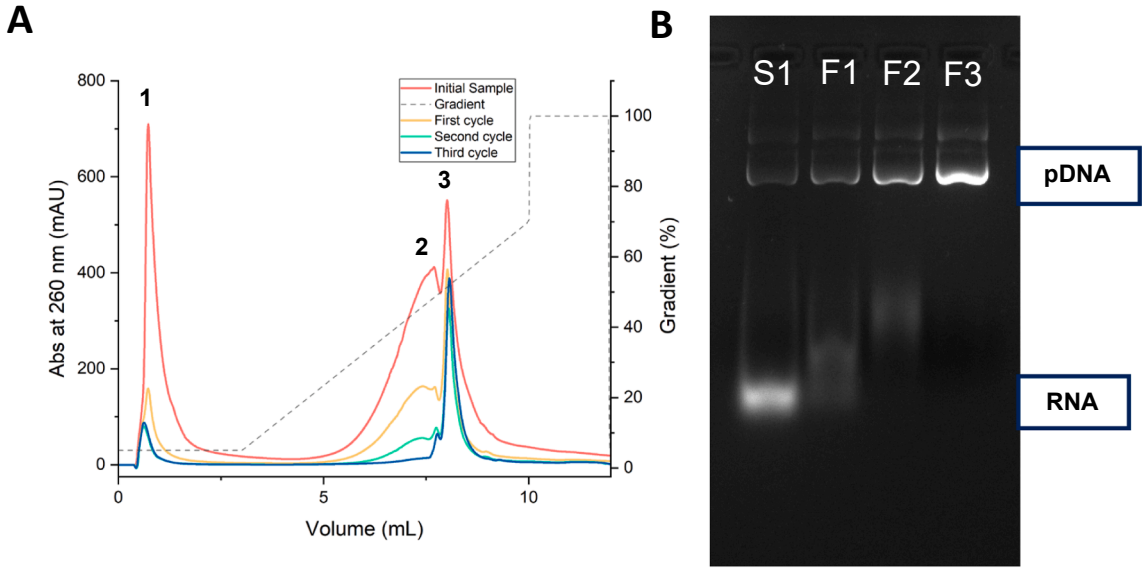

Fig. 8. Analysis of *E. coli* lysate and pDNA clarified samples subjected to the clarification procedure with < 10 MWCNTs, throughout three consecutive cycles (n = 3): A. Representative chromatograms (for the meaning of the numbers 1 to 3 see text); B. Agarose gel electrophoresis. S1 - Initial *E. coli* lysate sample; F1 – Supernatant recovered from the first clarification cycle, comprising all solutes not adsorbed onto MWCNTs; F2 - Supernatant after second consecutive cycle, comprising all solutes not adsorbed onto MWCNTs; F3 - Supernatant after third consecutive cycle, comprising all solutes not adsorbed onto MWCNTs.

Table 3
Quantitative analysis of genomic DNA and protein content in the lysate and clarified samples after < 10 MWCNTs adsorption procedure for three consecutive cycles (n = 3).

	Initial Lysate Sample	Composition of Clarified pDNA Sample:		
		1st cycle	2nd cycle	3rd cycle
[gDNA] (μg/mL)	523.3	313.3	206.7	90.0
[Proteins] (μg/mL)	128.5	27.3	11.2	5.4

Overall, through MWCNTs application in pDNA clarification, it achieved a significant reduction in RNA, gDNA, and proteins, and despite being described as a clarification step, the reduction on impurities level can significantly simplify the subsequent purification stage.

Considering this global analysis, it is possible to visualize the impact of this innovative clarification procedure on generating a highly pDNA-enriched sample (Fig. 8). Table 4 summarizes the guidelines set forth by regulatory agencies, namely FDA (Food and Drug Administration) and EMA (European Medicines Agency), to assure the quality, safety and efficacy of pDNA-based products [48,49]. With this clarification method, it is possible to reduce significantly the main impurities associated with pDNA biopharmaceutical products, facilitating the following polishing step. Moreover, and as referenced in the literature, the intermediate recovery step has the main objective of clarifying impurities, like RNA and proteins, that correspond to more than 90 % of the total solutes. The final goal is to end up with a solution where pDNA accounts for approximately 50 %, reducing the burden imposed on high-performance/high-cost unit operations [12]. By integrating the peaks from the chromatograms shown in Fig. 8A, it is achieved a reduction of 83.6 % in the total area, comparing the initial lysate sample with the sample recovered from the third cycle, as a consequence of the elimination of impurities throughout the clarification cycles. Overall, these results validate the potential of this platform as an effective DNA clarification method.

Table 4
Suggested criteria for pDNA-based vaccines from regulatory agencies, FDA (Food and Drug Administration) and EMA (European Medicines Agency) ([17,49–51]).

Impurities	Specifications
Proteins	<1%
gDNA	<1%
RNA	<1%
Endotoxins	40 EU/mg plasmid
Microorganisms	<1 CFU

(EU – Endotoxin unit; CFU – Colony-forming unit).

3.5. MWCNTs cytotoxicity

Considering the primary goal of this work, regarding the establishment of conditions that enable the isolation and clarification of plasmids that could potentially be used as biopharmaceuticals, it is essential to discard any cytotoxic effect of < 10 MWCNTs in the cells. The presence of adsorbent material in the final pDNA-containing sample is not expected. Still, assessing the cytotoxicity of the MWCNTs is crucial to ensure the safety of the processes, even if some remaining material is found in the pDNA sample. In this sense, the MTT assay was used to evaluate the NHDF cell viability in the presence of MWCNTs in three different amounts 25, 50, and 100 μg. The use of a considerably high quantity of MWCNTs was intended to confirm the safety of the material and method. Cells were exposed to these MWCNTs conditions for 24 and 48 h. The results presented in Fig. 9 demonstrate that MWCNTs did not induce any cytotoxic effect on these cells. Even using 100 μg of MWCNTs, the viability of cells remained around 86.7 % at 24 h and 80.3 % at 48 h, confirming the non-cytotoxic behavior of MWCNTs and the safety of this clarification/pre-purification step.

4. Conclusions

The exponential interest in pDNA-based therapies emphasized the eminent demand for developing efficient purification strategies to obtain this biomolecule with high purity while maintaining its integrity and biological activity.

Pristine MWCNTs emerged as novel solid supports to promote the fast and efficient clarification of pDNA from a complex sample. The

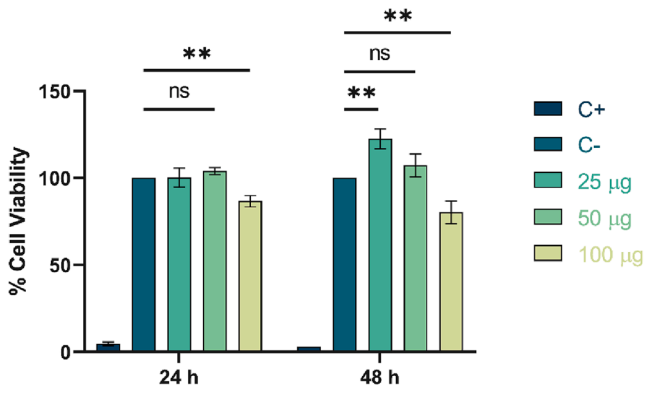

Fig. 9. Human fibroblast viability determined by MTT assay after 24- and 48-hours incubation with 25, 50, and 100 µg of pristine < 10 MWCNTs (mean ± SD, n = 3). The negative control (C-) comprised untreated cells, and the positive control (C +) was treated with ethanol 70 %. The viability percentage is expressed relative to the control cells. Statistical analysis was performed using "One-way ANOVA." Significant differences are indicated as: (ns = p greater than 0.05; **** $p \leq 0.0001$; *** $p \leq 0.001$; ** $p \leq 0.01$; * $p \leq 0.05$); and determined with Tukey's multiple comparisons.

described protocol removes all RNA and a significant fraction of proteins and gDNA from an *E. coli* clarified lysate, reducing the number of steps and time spent in downstream processes.

MWCNTs with < 10 nm of diameter demonstrate an impressive high adsorption capacity. Moreover, it was verified that RNA adsorption mainly depended on the hydrophobic interactions between the nitrogen bases of RNA and the aromatic surface of MWCNTs, leading to the preferred adsorption of single-stranded nucleic acids with more exposed bases, as is the case of RNA in comparison to pDNA.

It follows that MWCNTs without surface modifications can be used to clarify the target pDNA with high selectivity and binding capacity. Another advantage of this procedure over the ones already established for nucleic acid extraction is that no toxic solvents (such as chloroform and phenol) or animal-origin enzymes (ribonuclease A, proteinase K, and lysozyme) were used to isolate the pDNA. Thus, contributing to a more sustainable, greener, and safer clarification method. Overall, the findings of this work underlie the potential to improve the downstream processing of pDNA biopharmaceuticals.

CRediT authorship contribution statement

P. Ferreira: Conceptualization, Methodology, Investigation, Validation, Writing – original draft. **M. Riscado:** Conceptualization, Methodology, Investigation, Validation, Writing – original draft. **S. Bernardo:** Conceptualization, Methodology, Investigation, Validation, Writing – original draft. **M.G. Freire:** Conceptualization, Methodology, Resources, Writing – review & editing, Supervision, Project administration, Funding acquisition. **J.L. Faria:** Conceptualization, Methodology, Resources, Writing – review & editing, Project administration, Funding acquisition. **APM. Tavares:** Conceptualization, Methodology, Resources, Writing – review & editing, Supervision, Project administration, Funding acquisition. **CG. Silva:** Conceptualization, Methodology, Resources, Writing – review & editing, Supervision, Project administration, Funding acquisition. **F. Sousa:** Conceptualization, Methodology, Resources, Writing – review & editing, Supervision, Project administration, Funding acquisition.

Declaration of Competing Interest

The authors declare the following financial interests/personal relationships which may be considered as potential competing interests: [Fani Sousa reports financial support was provided by Foundation for Science and Technology. Pedro Ferreira reports financial support was provided by Foundation for Science and Technology. Micaela Riscado reports financial support was provided by Foundation for Science and Technology. Ana Paula Tavares reports financial support was provided by Foundation for Science and Technology. Mara G. Freire is member of the Editorial Board of Separation and Purification Technology.].

Data availability

Data will be made available on request.

Acknowledgments

The authors thank Dr. Thomas Roberts for providing the pcDNA3–FLAG–p53 construct through Addgene, ref.: 10838. This work was supported by the project PTDC/BII-BBF/29496/2017, funded by FEDER, through COMPETE2020-POCI and by national funds, through FCT/MCTES. The authors also acknowledge the projects UIDB/00709/2020, UIDP/00709/2020, UIDB/50011/2020 and UIDP/50011/2020, UIDB/50020/2020 and UIDP/50020/2020, and LA/P/0045/2020 (ALiCE) and LA/P/0006/2020 (CICECO) financed by national funds through FCT/MCTES (PIDDAC). Pedro Ferreira, Micaela Riscado, and A. P.M. Tavares acknowledge FCT for the PhD fellowships (2022.13803. BD), (2021.07658.BD), and the research contract CEEC-IND/2020/01867, respectively.

Appendix A. Supplementary material

Supplementary data to this article can be found online at https://doi.org/10.1016/j.seppur.2023.124224.

References

[1] T. Friedmann, R. Roblin, Gene Therapy for Human Genetic Disease? Science 175 (4025) (1972) 949–955.
[2] J.A. Kulkarni, et al., The current landscape of nucleic acid therapeutics, Nat. Nanotechnol. 16 (6) (2021) 630–643.
[3] J.J. Rossi, D. Rossi, Oligonucleotides and the COVID-19 Pandemic: A Perspective, Nucleic Acid Ther. 30 (3) (2020) 129–132.
[4] D. Hobernik, M. Bros, DNA Vaccines—How Far From Clinical Use? Int. J. Mol. Sci. 19 (11) (2018) 3605.
[5] B. Yang, et al., DNA vaccine for cancer immunotherapy, Hum. Vaccin. Immunother. 10 (11) (2014) 3153–3164.
[6] S. Scheiblhofer, J. Thalhamer, R. Weiss, DNA and mRNA vaccination against allergies, Pediatr. Allergy Immunol. 29 (7) (2018) 679–688.
[7] N. Zhang, K.S. Nandakumar, Recent advances in the development of vaccines for chronic inflammatory autoimmune diseases, Vaccine 36 (23) (2018) 3208–3220.
[8] J.N. Maslow, Vaccines for emerging infectious diseases: Lessons from MERS coronavirus and Zika virus, Hum. Vaccin. Immunother. 13 (12) (2017) 2918–2930.
[9] C. Sheridan, First COVID-19 DNA vaccine approved, others in hot pursuit, Nat. Biotechnol. (2021) 1479–1482.
[10] D.M.F. Prazeres, G.A. Monteiro, Plasmid Biopharmaceuticals, Microbiol. Spectr 2 (2014) 6.
[11] A. Abdulrahman, A. Ghanem, Recent advances in chromatographic purification of plasmid DNA for gene therapy and DNA vaccines: A review, Anal. Chim. Acta 1025 (2018) 41–57.
[12] D.M.F. Prazeres, Plasmid biopharmaceuticals: basics, applications, and manufacturing, John Wiley & Sons, 2011.
[13] J. Stadler, R. Lemmens, T. Nyhammar, Plasmid DNA purification, J. Gene Med. 6 (S1) (2004) S54–S66.
[14] M. Ghaemi, G. Absalan, Study on the adsorption of DNA on Fe3O4 nanoparticles and on ionic liquid-modified Fe3O4 nanoparticles, Microchim. Acta 181 (1–2) (2014) 45–53.
[15] A. Ghanem, R. Healey, F.G. Adly, Current trends in separation of plasmid DNA vaccines: A review, Anal. Chim. Acta 760 (2013) 1–15.
[16] S. Cardoso, et al., Arginine homopeptides for plasmid DNA purification using monolithic supports, J. Chromatogr. B 1087–1088 (2018) 149–157.
[17] C.P.A. Alves, D.M.F. Prazeres, G.A. Monteiro, *Minicircle Biopharmaceuticals–An Overview of Purification Strategies.* Frontiers, Chem. Eng. (2021) 2.
[18] C. Herrero Latorre, et al., Carbon nanotubes as solid-phase extraction sorbents prior to atomic spectrometric determination of metal species: A review, Anal. Chim. Acta 749 (2012) 16–35.
[19] L. Liu, et al., A simple and efficient method for the extraction and purification of tuberostemonine from Stemonae Radix using an amide group-based monolithic cartridge, Sep. Purif. Technol. 300 (2022), 121843.
[20] A. Andrade-Eiroa, et al., Solid-phase extraction of organic compounds: A critical review (Part I), TrAC Trends Anal. Chem. 80 (2016) 641–654.

[21] D. Tan, et al., Wearable bistable triboelectric nanogenerator for harvesting torsional vibration energy from human motion, Nano Energy 109 (2023), 108315.
[22] N. Kong, et al., Enriching Fe3O4@MoS2 composites in surface layer to fabricate polyethersulfone (PES) composite membrane: The improved performance and mechanisms, Sep. Purif. Technol. 302 (2022), 122178.
[23] B. Li, et al., A novel method integrating response surface method with artificial neural network to optimize membrane fabrication for wastewater treatment, J. Clean. Prod. 376 (2022), 134236.
[24] Z. Huang, et al., Fabrication of fibrous MXene nanoribbons (MNRs) membrane with efficient performance for oil-water separation, J. Membr. Sci. 661 (2022), 120949.
[25] Kaur, J., G.S. Gill, and K. Jeet, *Chapter 5 - Applications of Carbon Nanotubes in Drug Delivery: A Comprehensive Review*, in *Characterization and Biology of Nanomaterials for Drug Delivery*, S.S. Mohapatra, et al., Editors. 2019, Elsevier. p. 113-135.
[26] V. Negri, et al., Carbon Nanotubes in Biomedicine, Top Curr Chem (Cham) 378 (1) (2020) 15.
[27] W. Zhao, et al., Preparation and characteristics of a magnetic carbon nanotube adsorbent: Its efficient adsorption and recoverable performances, Sep. Purif. Technol. 257 (2021), 117917.
[28] G. Jian, et al., Applications of carbon-based materials in solid phase microextraction: a review, Carbon Lett. 24 (2017) 10–17.
[29] S. Yang, et al., Enhanced adsorption of Congo red dye by functionalized carbon nanotube/mixed metal oxides nanocomposites derived from layered double hydroxide precursor, Chem. Eng. J. 275 (2015) 315–321.
[30] E.D.V. Duarte, et al., Adsorption of pharmaceutical products from aqueous solutions on functionalized carbon nanotubes by conventional and green methods: A critical review, J. Clean. Prod. 372 (2022), 133743.
[31] P. Kumar, et al., Sorption behaviour of Pu4+ and PuO22+ on amido amine-functionalized carbon nanotubes: experimental and computational study, RSC Adv. 6 (108) (2016) 107011–107020.
[32] J. Chen, et al., Magnetic multiwall carbon nanotubes modified with dual hydroxy functional ionic liquid for the solid-phase extraction of protein, Analyst 140 (10) (2015) 3474–3483.
[33] K. Xu, et al., Solid-phase extraction of DNA by using a composite prepared from multiwalled carbon nanotubes, chitosan, Fe3O4 and a poly(ethylene glycol)-based deep eutectic solvent, Microchim. Acta 184 (10) (2017) 4133–4140.
[34] L.L. Hu, et al., Polyethyleneimine-iron phosphate nanocomposite as a promising adsorbent for the isolation of DNA, Talanta 132 (2015) 857–863.
[35] Ç. Kip, et al., Isolation of RNA and beta-NAD by phenylboronic acid functionalized, monodisperse-porous silica microspheres as sorbent in batch and microfluidic boronate affinity systems, Colloids Surf. B Biointerfaces 174 (2019) 333–342.
[36] S. Senel, Boronic acid carrying (2-hydroxyethylmethacrylate)-based membranes for isolation of RNA, Colloids Surf. A Physicochem. Eng. Asp. 219 (1) (2003) 17–23.
[37] Y. Fu, Q. Chen, L. Jia, RNase-free RNA removal and DNA purification by functionalized magnetic particles, Sep. Purif. Technol. 267 (2021), 118616.
[38] P. Pereira, et al., Advances in time course extracellular production of human pre-miR-29b from Rhodovulum sulfidophilum, Appl. Microbiol. Biotechnol. 100 (8) (2016) 3723–3734.
[39] O. Gjoerup, D. Zaveri, T.M. Roberts, Induction of p53-independent apoptosis by simian virus 40 small t antigen, J Virol 75 (19) (2001) 9142–9155.
[40] M.M. Diogo, et al., Purification of a cystic fibrosis plasmid vector for gene therapy using hydrophobic interaction chromatography, Biotechnol. Bioeng. 68 (5) (2000) 576–583.
[41] P. Chomczynski, N. Sacchi, Single-step method of RNA isolation by acid guanidinium thiocyanate-phenol-chloroform extraction, Anal Biochem 162 (1) (1987) 156–159.
[42] Sun, Y., et al., *2.47 - Adsorption and Chromatography*, in *Comprehensive Biotechnology (Second Edition)*, M. Moo-Young, Editor. 2011, Academic Press: Burlington. p. 665-679.
[43] M. Sianipar, et al., Functionalized carbon nanotube (CNT) membrane: progress and challenges, RSC Adv. 7 (81) (2017) 51175–51198.
[44] P. Li, et al., High-efficient nucleic acid separation from animal tissue samples via surface modified magnetic nanoparticles, Sep. Purif. Technol. 262 (2021), 118348.
[45] B. Nandy, M. Santosh, P.K. Maiti, Interaction of nucleic acids with carbon nanotubes and dendrimers, J. Biosci. 37 (3) (2012) 457–474.
[46] K. Pilely, et al., Monitoring process-related impurities in biologics-host cell protein analysis, Anal. Bioanal. Chem. 414 (2) (2022) 747–758.
[47] X. Zhou, et al., Design, preparation and measurement of protein/CNTs hybrids: A concise review, J. Mater. Sci. Technol. 46 (2020) 74–87.
[48] *Guideline on the quality, non-clinical and clinical aspects of gene therapy medicinal products.*, R.E.M. Agency, 2018, EMA - Committee for Advanced Therapies.
[49] *Guidance for industry: considerations for plasmid DNA vaccines for infectious disease indications*, New York, Food and Drug Administration, 2007, FDA - Center for Biologics Evaluation and Research.
[50] J. Urthaler, et al., Industrial Manufacturing of Plasmid-DNA Products for Gene Vaccination and Therapy, in: J. Thalhamer, R. Weiss, S. Scheiblhofer (Eds.), Gene Vaccines, Springer Vienna, Vienna, 2012, pp. 311–330.
[51] M. Schleef, et al., Production of non viral DNA vectors, Curr. Gene Ther. 10 (6) (2010) 487–507.